

POLYOCTANEDIOL CITRATE-ZINC OXIDE NANO-COMPOSITE MULTIFUNCTIONAL TISSUE ENGINEERING SCAFFOLDS WITH ANTI- BACTERIAL PROPERTIES

E. H. MIRZA^{a, b}, W. MOHD AZHAR BIN WAN IBRAHIM^a, B. PINGGUAN-MURPHY^a, I. DJORDJEVIC^{a*}

^a*Department of Biomedical Engineering, Faculty of Engineering, University of Malaya, Kuala Lumpur 50603, Malaysia.*

^b*Department of Biomedical Technology, College of Applied Medical Sciences, King Saud University, Riyadh, Kingdom of Saudi Arabia*

In this paper we report the processing and characterization of composite scaffolds made from polyoctanediol citrate (POC) polyester elastomer and zinc oxide nanoparticles (ZnO NPs). The composite scaffolds, with varying concentration of ZnO, were fabricated by solvent-casting/particulate-leaching technique. In order to investigate the fundamental surface properties of POC-ZnO nano-composite material, we have developed thin films produced by spin-coating technique. Both scaffolds and coatings have been analysed for their surface morphology, wettability, mechanical and structural properties, *in vitro* ion release kinetics and anti-bacterial characteristics. We demonstrate that the material properties can be successfully controlled by simple variation of NP concentration within the composite. The ion release kinetics from POC-ZnO scaffolds is strongly dependent on NP concentration and degradation of pure POC matrix. All the composite scaffolds have shown strong antibacterial characteristics however, cell culture studies demonstrated that 1 % ZnO incorporation in POC polymer is the optimal concentration for chondrocyte cells. In comparison to pure POC scaffold, a relatively low concentration of NP (1% composite) has shown unusual stimulation of cell proliferation within the porous structure. The presence of ZnO in low concentrations not only prevents bacterial adhesion but also stimulates growth of healthy cells. This result is of major importance for development of multifunctional scaffolds based on biodegradable polyesters.

(Received March 3, 2015; Accepted April 24, 2015)

Keywords: Elastomeric scaffolds; Citric acid; Nano-composite; ZnO nanoparticles; Anti-bacterial properties.

1. Introduction

Tissue engineering strategies utilize polymeric scaffolds that serve as a temporary extracellular matrix (ECM) for seeded cells [1-4]. The adopted strategy is that scaffold should biologically degrade over time, leaving a fully developed and functional tissue. Production of tissues may be accomplished *in vitro*, where cell-seeded scaffolds are placed in bioreactors, or *in vivo*, where the cell/scaffold “composite” is surgically placed inside the human body. The latter is of particular interest in the development of multifunctional advanced materials for scaffolds fabrication. Every surgical implantation of biomaterials (or medical devices) requires tissue incision and therefore serious consideration must be given to control of infections. Apart from necessary support for tissue growth, scaffolds should also possess antibacterial properties in order to battle serious problems related to scaffold implantation.

Drug delivery devices are generally considered to be an effective route for administration of bio-active substances to the site of implantation. Postoperative infections are a major threat and

*Corresponding author. ivandjordjevich@hotmail.com

a challenging issue that may have deleterious effects on the patient's life [5, 6]. Various intrusions that are presently carried out, and which are focused on minimizing the risk of infections, include prophylactic antibiotics as well as the treatments prior to surgical intervention. Those treatments include: ultra-violet exposure [7, 8], povidone-iodine lavage [9], antibiotic irrigation [8] and laminar airflow [10]. Infection risk is closely linked to initial bacterial attachment and subsequent proliferation on the implants surface. The bacteria adhere, forming a layer, more commonly known as "biofilm". These biofilms are even resistant to antibiotics and the host immune system, and therefore treatment requires more vigorous measures [11]. For that reason it is essential to prevent initial bacterial attachment on the implant surface.

One of the materials that have proven to be effective against bacteria in general is zinc oxide (ZnO). This substance is currently considered a Generally Recognized as Safe (GRAS) material, approved by the Food and Drug Administration (FDA) [12]. Furthermore, ZnO can be fabricated into nanoparticles (NPs) [13-15], that can be embedded inside a biodegradable polymer matrix and subsequently released in a highly controlled manner. Polyoctanediol citrate (POC) elastomer is one of the prominent new materials for scaffold fabrication [16-18]. POC and other types of citric acid (CA)-based elastomers have shown excellent performance in various biomaterial applications, including scaffolds for soft tissue engineering, biodegradable bone fixation devices and drug delivery devices [19-21].

In present paper we report material characteristics of newly-developed POC-ZnO scaffolds produced by well-established solvent-casting/particulate-leaching technique. Tissue engineering applications require three-dimensional structures with high level of porosity and pore sizes in the range of 100-200 μ m. In many cases such porous structures alter material properties that were originally recorded for sample films [22, 23]. Apart from antibacterial properties of the POC-ZnO composite, the scaffolds must be investigated for their potential support of cellular growth, proliferation and toxicity. Similar to other polymer/solid composites the presence of ZnO NPs mechanically enforces the scaffold thus providing necessary toughness for engineering of hard tissues. In particular, our target is to explore the possibility for using POC-ZnO nano-composite scaffolds for engineering of cartilage tissue. We prepared POC-ZnO nano-composite scaffolds with variation of ZnO concentration and a series of experiments was conducted in order to: (i) investigate the influence of ZnO concentration on material characteristics; (ii) establish bactericidal properties by measuring the proliferation rate of *Escherichia coli* and *Staphylococcus aureus*; and (iii) examine the bioactivity, biocompatibility and potential of POC-ZnO scaffolds for cartilage tissue engineering by *in vitro* experiments with primary bovine chondrocyte cells.

2. Materials & Methods

2.1 Materials

1, 8-Octanediol (OD), citric acid (CA), nano-ZnO, 1, 4-dioxane, phosphate buffer saline (PBS), Luria Bertani (LB) broth powder and LB agar powder were purchased from Sigma-Aldrich Malaysia. Sodium chloride (NaCl) was purchased from Fisher Scientific Malaysia, and Teflon moulds (60mm diameter by 15mm depth) were custom designed. Bacteria *E. Coli* (ATCC 15597) and *S. Aureus* (NCTC 6571) were purchased from Microbiologics®. Dulbecco's Modified Eagle's Medium (DMEM) was purchased from Corning and foetal Bovine Serum (FBS) from Gibco by Life Technologies. L-glutamate and Hepes buffer was supplied from Biowest. Antibiotic-Antimycotic was purchased from Cellgro while L-ascorbic acid was purchased from System.

2.2 Synthesis of pre-polymer and preparation of scaffolds, films and coatings

POC was synthesized by a previously reported method of melt polyesterification between CA and OD monomers [24]. After the reaction was completed the product in the form of pre-polymer was then taken out in a glass petri dish and stored at 4 – 8 $^{\circ}$ C until further use. Pure-POC scaffold and 3 different POC-ZnO composite scaffolds with varying w/w percentages of ZnO NPs (1%, 3% and 5%) were prepared. All scaffolds were prepared by the following method: POC pre-

polymer was dissolved in dioxane (50% w/v) and the pre-calculated amounts of ZnO (1%, 3% and 5% w/w with respect to weight of the pure pre-polymer) were added to POC solutions. The POZ-ZnO-dioxan mixtures were sonicated for 10 minutes. After that, sieved NaCl crystals of size 200 – 300 μ m were added to the POC-ZnO mixture (NaCl/POC-ZnO = 9:1). The composite POC-ZnO-NaCl-dioxane slurry was poured in TeflonTM moulds and placed for solvent evaporation and curing at 80⁰C for 1 week. Following the curing period, the solidified blocks of each of four samples were removed from TeflonTM moulds and placed in a custom designed rack to leach out the salt with sequential progressions in distilled water for 5 days at room temperature. Scaffolds were frozen and sliced cut (~ 6 mm thickness; Figure. 1). The slices were further cut using a cork borer to produce cylinder-shape samples with 6 mm in diameter. All samples were freeze-dried for 24 hours and were kept in a desiccator until further use. Pure-POC Scaffold was used as control in all measurements. For water-in-air contact angle experiments, POC control and POC-ZnO (50% w/v in dioxane) solutions were spin-coated on microscope cover slips, using Laurell (WS-650MZ-23NPP) spin coater. Glass cover slips were placed in the coating chamber and the slide was spun at 3000 rpm for 10 seconds. Each time 6 drops of solution was dropped at the centre of the glass slip. The process was repeated 3 times for each slide. Coated cover slips were placed flat in the oven at 80⁰C for pre-polymer curing and solvent evaporation for 1 week. Swelling tests were performed on composite films prepared by a solvent casting technique (Fig. 1).

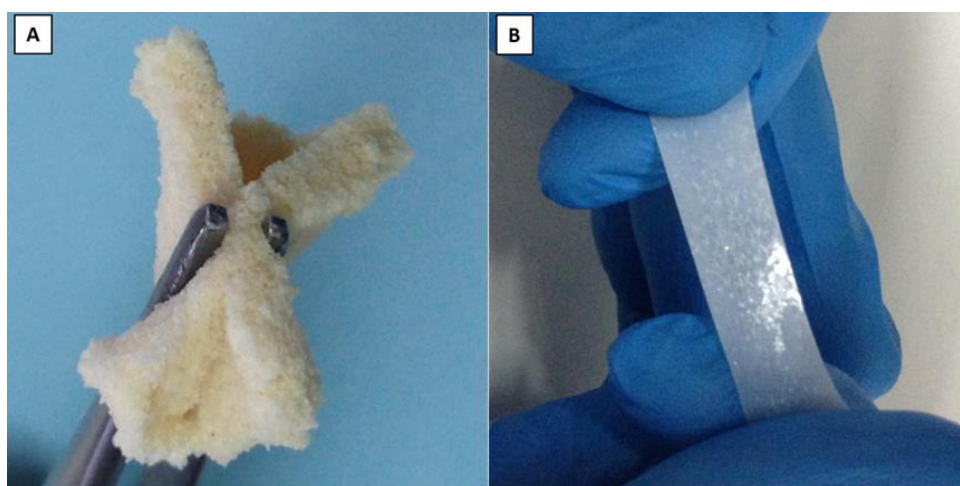


Fig. 1. Digital photograph of representative POC-ZnO composite sample: (A) 3% POC-ZnO porous scaffold produced by solvent-casting/particulate leaching technique; (B) 3% POC-ZnO film used for swelling in water experiment, produced by solvent casting technique (~ 1 mm-thickness).

2.3.2 Contact angle experiment

Water-in-air contact angle of the polymer coatings was measured by sessile drop method at room temperature. The experiment was performed using a Contact Angle System OCA instrument and imaging system (OCA 20, DataPhysics Instruments GmbH, Filderstadt, Germany). The contact angle was measured within 1 min after a drop of water (2 μ l) was placed on the composite-coated slide. Three coated slides of each composition (POC-ZnO, 1%, 3%, 5% and POC control) were used. Each measurement was taken on 5 different polymer coated glass slides and the contact angle readings were recorded on three different locations of each slide. The results were averaged and the data are presented with standard deviations.

2.3.3 Mechanical properties

The compression tests were performed on POC-ZnO scaffolds using Instron mechanical tester (Instron Microtester 5848, Instron Corp., Norwood, MA, USA) equipped with a 2kN load

cell. Scaffolds were cut in cylindrical shapes (6 mm-diameter / 6 mm-height) and subjected to 50 % compression at a rate of 1 mm/min. For percentage recovery, the height of each cylindrical scaffold was measured 2 min after applied compression (n= 5). Porosity of the scaffolds (n=5) was measured with the Archimedes principle with a custom designed setup as reported previously by our group [25].

2.3.4 Infra-red spectroscopy analysis

Fourier transform infrared spectra were obtained for the scaffolds using spectrophotometer-Thermo Scientific Nicolet iS10 (Thermo Fisher Scientific, Waltham, MA, USA) operating in attenuated total reflectance mode (ATR-FTIR) at room temperature, within a wavelength range of 450 – 4000 cm^{-1} .

2.3.5 Thermal analysis

Thermo gravimetric analysis (TGA) was performed on all the scaffolds within a temperature range of 30-900 °C at a rate of 10 °C/min using PerkinElmer, TGA 4000 (PerkinElmer, Waltham, MA, USA). The onset of degradation temperature was measured after 10 % of degradation.

2.3.6 Swelling experiment

Swelling in water degree was measured for composite discs (6 mm-diameter / 1 mm-height; Figure. 1) produced by solvent casting. Samples were placed in 10 ml of distilled water and the polymer films (produced by solvent casting) were taken out at different time points. Their weight was measured after lightly cleaning their surface with lint-free paper. Percentage swelling was calculated as follows: swelling % = $[(W_s - W_o) / W_o] \times 100$; where W_s is the weight of the swollen polymer disk at each time point and W_o is samples' dry weight.

2.3.7 ZnO NPs release kinetics in physiological conditions

To observe the release of ZnO NPs, cylindrical scaffolds (6 mm-diameter / 2 mm-thickness) were placed in 10 ml of PBS in conical tubes and kept at 37°C throughout the whole experiment. 2 ml of solution from each conical tube was withdrawn at each time point (day 1, 7, 14 & 28) and was kept at 4 – 8°C until the analysis. The concentration of Zn^{2+} (ppm) was detected by atomic emission spectroscopy (AAS) using Agilent 4100 (Agilent Technologies, Inc., Santa Clara, CA, USA) microwave plasma-atomic emission spectrophotometer (MP-AES). The standard for Zn^{2+} was purchased from Sigma-Aldrich Malaysia.

2.3.8 Anti-bacterial properties for Gram positive and Gram negative bacteria

Antibacterial test for scaffolds in direct contact with the bacteria was performed by liquid culture method. Rectangular strips of POC-ZnO polymer composite were cut (30 mm x 10 mm x 5 mm) and placed in 15 ml conical tubes with 10 ml of LB broth inoculated with 50 μl of 10^{4-5} CFU/ml *E. Coli* (ATCC 15597) and *S. Aureus* (NCTC 6571). Samples were placed in shaking incubator at 37°C with a speed of 50 rpm. Pure-POC scaffold and LB broth (without any scaffold) were inoculated with similar bacterial densities and were used as positive and negative controls respectively. The optical density was measured at 595 nm every 2 hours (for 8 hours) with microplate reader (BMG LABTECH, Offenburg, Germany).

2.3.9 In vitro tests with chondrocyte cell culture

All polymer composite scaffolds were tested for their cytotoxicity towards bovine chondrocytes. Bovine legs of post-slaughtered cows were obtained up to carpal joint only. Bovine chondrocytes were isolated from metacarpal-phalangeal joints as described elsewhere [26, 27].

Cells were used when only greater than 95% viability was obtained. Toxicity was measured by resazurin reduction cell viability test. Scaffolds were autoclaved before cell seeding and then were allowed to neutralise in chondrocyte medium overnight. Scaffolds were then placed in 24 well plates and dried under laminar flow for an hour. A volume of 20 μ l cell suspension with a concentration of 3×10^7 cells/ml was spotted on top of scaffold. Cells were allowed to attach for 2 hours after which 2ml of medium/well was added. Reduction in resazurin was determined after 24 and 72 hours as described previously [28]. Briefly, medium was removed from the wells containing cell seeded scaffolds and then washed with PBS. One ml of resazurin was added to each well and then kept in the incubator for 4 hours at 37°C and 5% CO₂. After the incubation time the plate was wrapped in aluminium foil and was shaken at 30 RPM on a bench top shaker for 1 minute. From each well 100 μ l of resazurin solution was placed in 96-well plate and resazurin solution from unseeded scaffold was taken as blank. Absorbance was read through a microplate reader. Scaffolds with cells were taken out after periods of time and morphology of cells was observed by FESEM by using a standard protocol of cell fixation (formaldehyde) and gold coating.

2.3.10 Statistical analysis

Data is reported as means with their standard deviation. The data was taken to be significant with a confidence interval of 95% ($\alpha \leq 0.05$). Student's t-test was performed when comparing two groups while a two-way ANOVA was performed for comparing means of more than 2 groups at the same time.

3. Results and discussion

3.1 Surface morphology

Fig. 2 shows the FESEM images of prepared scaffolds. As expected the pores were formed in semi-rectangular shapes after leaching out the salt crystals. The pore sizes are in the range of 100-200 μ m, (which is smaller than dimensions of the sieved salt in the range of 200-300 μ m), consistent with previously reported results [29]. Most importantly, FESEM images reveal homogenous distribution of pores which is a desirable feature for optimal cell distribution after the seeding [30, 31]. In comparison to POC control (Figure. 2, A), addition of ZnO NPs did not have any significant impact on the pore size or pore structure that could be observed in FESEM experiment. Inserts in Figure. 2 are representative images of surfaces recorded inside the pores of produced scaffolds. With addition of ZnO NPs, there is a clear presence of ZnO NPs on the composite surface inside the pores (Figure. 2, A-D, inserts) which would most likely have an influence on both bactericidal properties and cell toxicity. Furthermore, EDX analysis confirmed the presence of Zn on the outermost surface layer and the detected amount of Zn on POC-ZnO surfaces was 0.49%, 1.64%, and 2.02 % for 1% POC-ZnO, 3% POC-ZnO and 5% POC-ZnO respectively. It is important to note that the increase in surface concentration of Zn corresponds to the pre-determined concentrations of ZnO NPs in composite scaffolds.

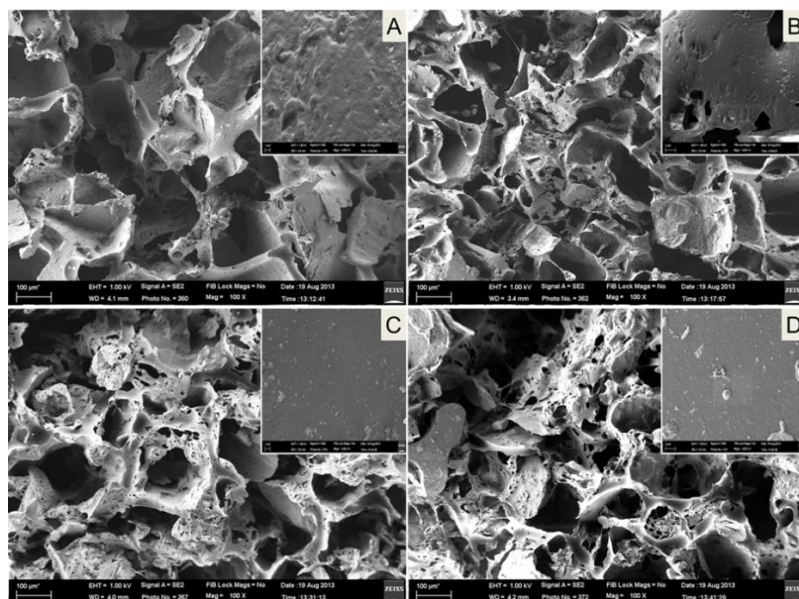


Fig. 2. FESEM images of POC (control) and POC-ZnO composite scaffolds: (A) POC; (B) 1% POC-ZnO; (C) 3% POC-ZnO; (D) 5% POC-ZnO; inserts show representative magnified surfaces of pore walls within scaffolds (inserts: A and B bars = 1 μm ; C and D bars = 2 μm).

3.2 Influence of surface ZnO NPs on relative hydrophilicity

Thin composite films were processed by spin-coating technique for wettability measurements and the surface morphologies of the samples (observed by optical microscopy) are shown in Figure. 3. In comparison to nano-composite coatings, pure POC shows polymer delamination from the glass surface and such irregular morphology could not be detected on composite coatings. The presence of ZnO NPs can be observed both on the surface of the films (Figure. 3, B) and within the bulk of the material (Figure. 3, C). We detected ZnO NP aggregates of 10-20 μm that could not be avoided in the current method [32]. In case of 1% POC-ZnO there is an obvious difference in surface concentration of ZnO, when compared to the other coatings. This result somehow opens a new possibility to develop nano-composite coatings with high level of control over surface composition.

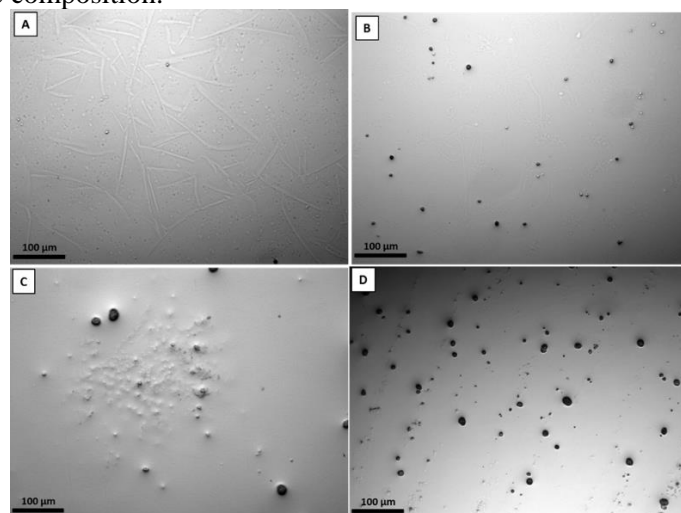


Fig. 3. Optical microscopy images of composite POC-ZnO surfaces developed by spin-coating technique: (A) POC; (B) 1% POC-ZnO; (C) 3% POC-ZnO; (D) 5% POC-ZnO.

Water-in-air contact angle values on polymer coated glass slides were measured to determine the effect of surface ZnO concentration on hydrophilicity and the results are shown in Figure. 4. Evidently, an increase in ZnO content results in more hydrophobic surfaces. There is no significant difference between contact angles measured for 3% and 5% POC-ZnO, although all composite coatings displayed a consistently higher contact angle values in comparison to hydrophilic POC. This implies that increasing the ZnO concentration increases the cohesive forces associated with bulk water more than that of the water with the surface [33]. Higher contact angles can also be attributed to increased surface roughness which results in trapped air between liquid and solid to cause greater repellence [34]. Such surface interactions with water are causing the more hydrophobic behaviour of the POC-ZnO composite material in comparison to POC control.

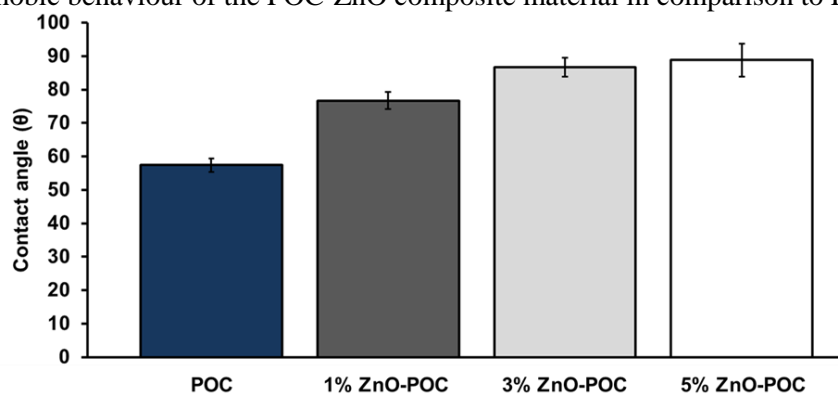


Fig. 4. Water-in-air contact angle results measured for thin POC-ZnO films produced by spin-coating technique.

3.3 Physical properties of POC-ZnO scaffolds: porosity and elasticity

Table 1 represents the porosities of POC and composite POC-ZnO scaffolds. The porosities for all the scaffolds are ranging from 82 to 86%; this implies that after salt leaching the actual porosities may drop 4-8% from expected value due to the recovery of the elastomeric material [29, 35].

Table 1. Compression properties and porosities of POC-ZnO scaffolds.

Scaffold	Compressive Modulus (MPa)	Recovery (%)	Porosity (%)
Pure-POC	0.243 ± 0.09	94.55 ± 2.52	82.91 ± 3.49
1% ZnO-POC	0.31 ± 0.10	91.94 ± 4.5	85.92 ± 2.41
3% ZnO-POC	0.537 ± 0.33	76.81 ± 4.82	86.01 ± 1.92
5% ZnO-POC	0.442 ± 0.23	60.66 ± 4.49	82.57 ± 7.33

We also found that the scaffolds can withstand stresses of up to 70 MPa at around 50% strain, which is far greater value than what a human tissues experience during normal activity [36, 37]. Judging from compression test alone, POC-ZnO scaffolds can find potential applications for load bearing tissues such as cartilage in knees and ankles. The compression moduli increase with increasing concentration of ZnO, expected for a contribution of the filler within the composite (Table 1). Overall, the analysed samples showed elastic nature which is an important feature in biomaterials research. If a degree of compressive elasticity can be judged from the recovery after stress, POC-ZnO scaffolds showed substantial variation for recovery within the range of 94-60 %. As the concentration of ZnO increases, the scaffolds tend to recover at a slower pace. This is most likely a result of agglomeration of ZnO NPs when mechanically loaded. Increased stiffness is

attributed to solid ZnO NPs and facilitated interaction between both phases of the composite. On the other hand, the addition of ZnO NPs increased the ductility, as previously described for other polymer nano-composites [38, 39]. Apart from the expected influence on mechanical properties by the presence of “filler” in polymer composite materials, ZnO is expected to show antibacterial, wound healing, and cell proliferating capabilities, which are the major attributes in current research [40, 41]. However, all tissues respond to physical properties of the biomaterial so the fundamental physical tests are necessary in order to establish sensitive and highly complex interactions at cell-biomaterial interfaces.

3.4 Chemical composition

The ATR-FTIR spectra for pure-POC and 5% POC-ZnO are shown in Figure 5. A broad peak at $\sim 1720\text{ cm}^{-1}$ (present in all samples) indicates successful polyesterification between CA and OD monomers [20]. Other POC-ZnO composites (1% and 3%) did not show any significant difference in comparison to POC scaffold [42, 43]. Peaks at 1630 cm^{-1} and 610 cm^{-1} indicate the presence of ZnO NPs within the POC matrix at the depth of several microns, detectable with ATR-FTIR.

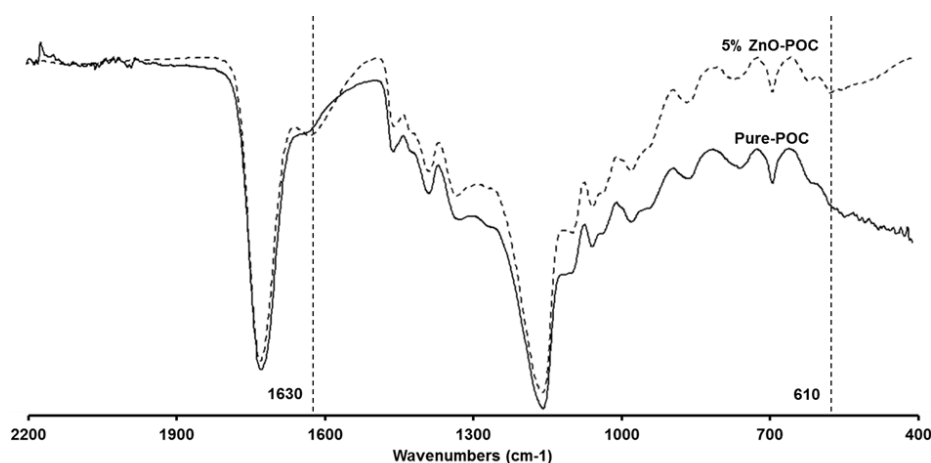


Fig. 5. Representative ATR-FTIR spectra of POC and 5% POC-ZnO scaffolds.

In our previous work we have examined films that were produced with higher concentrations of ZnO (2.5%, 5% and 10%) [22]. In case of the films (thickness: 1 mm) the intensities of peaks at 1630 cm^{-1} and 610 cm^{-1} were much more pronounced even for 2.5% and 5% POC-ZnO. This is most likely the consequence of porosity of scaffolds (in comparison to composite films) when measured in ATR mode. More accurate results can be obtained by analysis of polymer composite films with flat surface.

3.5 Thermal stability

Thermograms of all the scaffolds were recorded in TGA experiment. Figure 6 indicates a high stability and a high degree of polymerization without detection of low molecular weight residues. TGA results show a two-step thermal degradation process, recorded for all the examined samples. The onset of degradation (OD) was detected in the range of $200\text{--}220\text{ }^{\circ}\text{C}$, where POC has the lowest and 5% POC-ZnO the highest OD temperature, corresponding to the pre-determined concentrations of ZnO [29]. An important structural feature is that the thermal stability increases with increasing the concentration of ZnO in the POC-ZnO scaffolds. Such a feature is likely to influence other material properties such as swelling in water and release kinetics of ZnO from polymer matrix. The experiments were repeated for different sections of the scaffolds and the solid residue after complete degradation corresponded to ZnO concentrations within the composites

(Figure 6). This result proves the efficiency of the method and the even distribution of ZnO NPs over entire volume of the scaffolds.

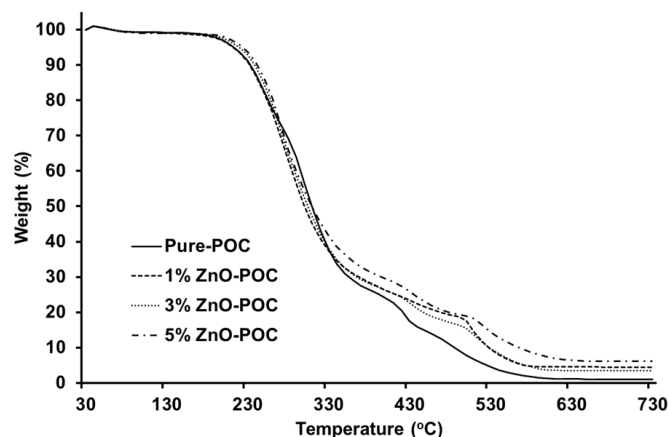


Fig. 6. Thermal degradation curves of produced scaffolds measured by TGA.

3.6 Swelling and cross-linking density

The results from swelling experiments are shown in Figure 7. The initial swelling rate in water was the same for all the tested films. After 1 h, a lower swelling rate was observed for POC and 1% POC-ZnO while other two composites showed a constant equilibrium percentage swelling (EPS). An obvious decrease in EPS after 6 hours is a result of increasing cross-linking density with ZnO concentration (Figure 7).

According to the rubber elasticity theory, Young's modulus is directly proportional to cross-linking density of elastomers. Therefore, the lowest swelling rate is expected to show highest value for Young's modulus (Table 1). Another important feature that could influence swelling behaviour is a relative hydrophylicity/hydrophobicity of developed composite materials. A significant increase in water contact angle (observed after addition of ZnO; Figure 4) also influences swelling behaviour. The hydrophobic component of the composite material (ZnO NPs) does not allow water to penetrate into the material and therefore causes decreased swelling [23]. This is an important result which would most likely influence the initial release of ZnO NPs from POC matrix and would subsequently influence different interactions with biological systems.

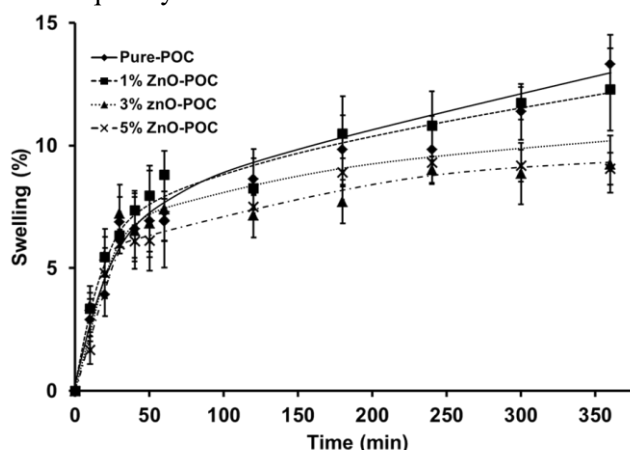


Fig. 7. Percentage swelling in water: POC and POC-ZnO composite films.

3.7 ZnO release kinetics

The release studies were performed in order to evaluate the relative concentration of Zn^{+2} ions from POC-ZnO scaffolds. Ion concentration was reasonably considered as directly proportional to the release of ZnO NPs into aqueous medium. This simulation of physiological

conditions (*in vitro*: 37 °C; PBS) is important in order to assess the scaffolds for future experiments with cell seeding and subsequent implantation *in vivo*. The release kinetics curves after 28 h are presented in Figure 8. Only after 7 days we could observe a relatively small difference in amount of ZnO released from POC-ZnO scaffolds. The relative concentration of Zn²⁺ after days 14 and 28, measured for 5% POC-ZnO was much higher in comparison to other two composites (Figure 8). The high concentration of ZnO inside the POC matrix (5%) caused a “burst release” between days 14 and 28, where the Zn²⁺ concentration doubled between two time points. As expected the lowest concentration of Zn²⁺ was detected for 1% POC-ZnO after 28 days. Unlike 5% POC-ZnO, both 1% and 3% POC-ZnO scaffolds maintained “zero order release kinetics” in the period of three weeks (between day 1 and day 28 in Figure 8) [44]. There are two possible mechanisms of ZnO NPs release from the POC matrix: (1) particle erosion after polymer swelling; and (2) polymer degradation and subsequent particle release.

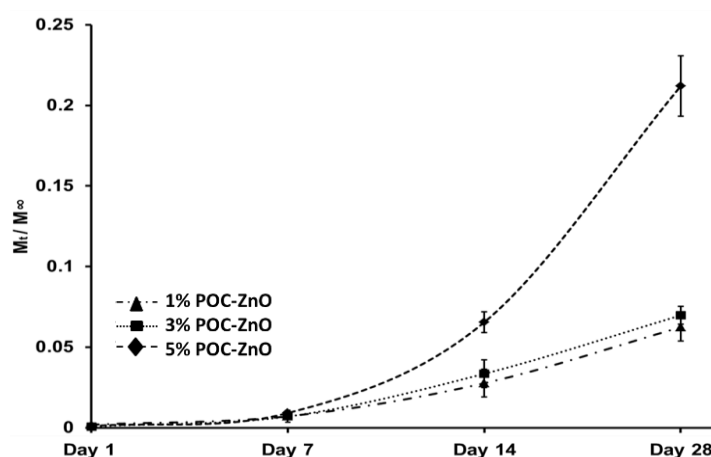


Fig. 8. In-vitro Release kinetics profile of ZnO (Zn²⁺) from POC-ZnO composites in PBS at 37°C; M_t = mass of ZnO released at time intervals; M_∞ = total mass of ZnO within the composite (all M_t/M_∞ ratios are the mean values for five samples measured with AAS).

Our results indicate that the most likely release mechanism is through degradation process. Since there was a minimal concentration of Zn²⁺ detected after 1 day it is less likely that swelling would have any influence on the release of ZnO (Figure 8). The degradation rate of POC can vary depending on the processing conditions, in particular, curing temperature, pressure and time has a strong influence on a cross-linking density and subsequent *in vitro* degradation properties of the final product [42]. POC reported in this paper substantially degrades in physiological conditions within the period of one month (70 % of degradation) [23]. For that reason it is expected for the amount of released particles to be proportional to the content of solids inside the composite. Since there is an evidence of strong anti-bacterial properties of ZnO, it is important to establish the correlation between ZnO release kinetics and influence on surrounding bacteria.

3.8 Anti-bacterial properties of POC-ZnO composite scaffolds and general discussion

Fig. 9 shows bacterial growth of *E. Coli* and *S. Aureus* in the presence of both POC and composite scaffolds over the period of 8 h. There is a possibility that small amounts of ZnO had been released into the surrounding medium due to the polymer swelling and thus caused the depletion of bacteria. From our results the amount of ZnO released after one day was below the detection limit and therefore such interpretations remain inconclusive. On the other hand, we have detected the highest concentration of Zn present on the surface of 5% POC-ZnO (Figure 3 and EDX results, section 3.1). Such result can be related to anti-bacterial test where the bacteria perish more rapidly in the presence of increasing surface concentration of ZnO (Figure 9). As mentioned before, ZnO is known to possess anti-bacterial properties. T. Jin et al. have tested ZnO NPs against various bacteria and it was suggested that ZnO particles should contact or penetrate bacterial cell

wall to demonstrate antibacterial behaviour [45]. For that reason ZnO NPs must come in contact with the bacteria in order to express their anti-bacterial behaviour. Our scaffolds showed ZnO NPs on the outermost surface layer (Figure 2 and Figure 3) which is a desirable feature that would help fighting infections and formation of biofilm by attached bacteria. Other polymer matrices have also been mixed with ZnO in order to produce the anti-bacterial composites. Zhang et al. have used ZnO NPs that was mixed with polyethylene glycol (PEG) and polyvinylpyrrolidone (PVP) as dispersants.

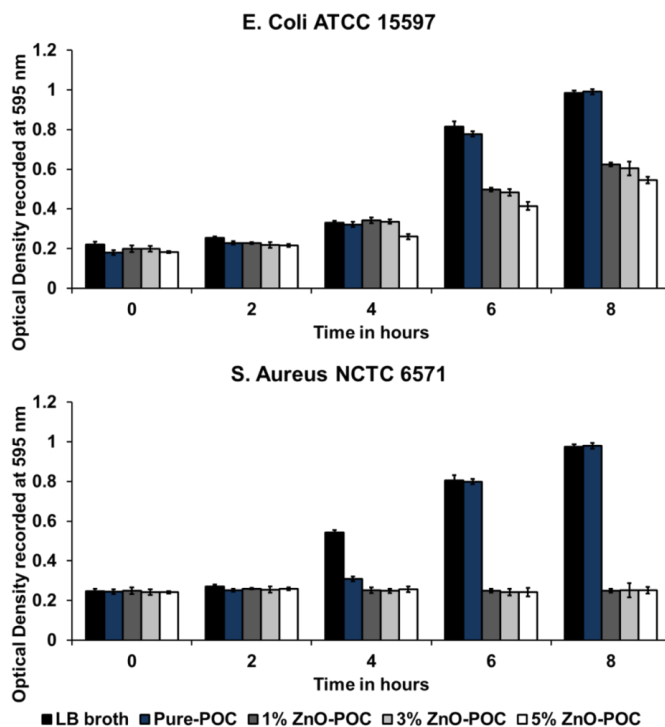


Fig. 9. Growth rates of *E. coli* and *S. Aureus* in LB broth inoculated with $50 \mu\text{l}$ of 10^{4-5} CFU/ml for POC (positive control), LB Broth (negative control) and POC-ZnO composite scaffolds (optical density at 595 nm was measured in microplate reader and is proportional to bacterial growth).

They reported that the antibacterial activity against *E. coli* increases with the increase in concentration of NPs (independent of particle size) [46]. To our knowledge, no attempt has been made to produce biodegradable tissue engineering scaffolds from CA-based polyester elastomer and ZnO NPs that would have strong anti-bacterial properties.

Biological systems are complex and ZnO NPs (or Zn^{2+} ions) can directly influence some processes. For example, Zn is attributed to cause a reduction in inflammation among cells by lowering oxidative stresses [47]. It has also been reported that Zn-deficient cells are more susceptible to DNA damage and development of cancer [48, 49]. In tissue engineering applications, different “bio-activity” factors must be considered, such as: (i) influence of released particles on the growth and proliferation of tissue-specific cells; (ii) particle influence on phenotype when stem cells are used; (iii) blood compatibility and inflammatory response; and (iv) biodegradation product of the polymer and physico-chemical interaction with ions in surrounding liquid medium (both *in vitro* and *in vivo*).

POC is known to have excellent biomaterial properties [16, 24]. The elastic nature and non-toxic components (used in preparation process) are the key features of POC and other CA-based elastomers. The addition of ZnO retains elastic nature (Table 1) and does not change the chemical composition of synthesised polymer (Figure 5). There are reasonable concerns about the influence of ZnO on cellular growth since ZnO effectively inhibits the growth of bacterial cells (Figure 9) [50]. However, the smallest amount of ZnO NPs has shown much better performance

than pure POC in terms bacterial inhibition (1%; Figure 9). This is possibly the key feature of POC-ZnO composite: material can be produced in the same fashion as POC with very important advantage over POC. The presence of ZnO enables anti-bacterial potential that would “shield” the implanted scaffold in both initial stages of implantation and over periods of bio-degradation time *in vivo*.

3.9 Compatibility with primary chondrocyte cells

Resazurin reduction results in (Figure 10, A) revealed that pure-POC and 1% POC-ZnO did not had any adverse effect on cell viability, however 3% and 5% POC-ZnO demonstrated highly cytotoxic behaviour towards primary bovine chondrocytes even after 24 hours. Similar results were reported by Feng Pei et.al where 3.5 wt% of ZnO in β -tricalcium phosphate scaffolds demonstrated cytotoxicity for MG-63 cells [51]. In the same study, 2.5 wt% of ZnO was reported to enhance osteoblast cell proliferation and increase cell viability. The scaffold matrix must be carefully considered in such system. Degradation rate, swelling and hydrophylicity of the polymer scaffold (or ceramic) must have a strong influence on particles release and therefore the influence on both bacteria and tissue specific cells. Another important aspect for biomaterials in general is the cellular morphology of adhered cells. In our study, FESEM images (Figure 10, B and C) reveal a healthy morphology of seeded chondrocytes, inside the scaffolds volume. In particular, nano-composite 1% POC-ZnO scaffold (Figure 10, C) is more uniformly covered by cells with spherical morphology characteristic for chondrocyte cells [52]. Cells on control scaffolds (POC) tend to be more fibroblastic which is a characteristic of monolayer cultures [53]. Another reason why cells on POC-ZnO composite showed more characteristic morphology is that NPs could provide anchorage to the cells and a rough surface that prevents the chondrocytes to change their morphology to fibroblasts [54, 55].

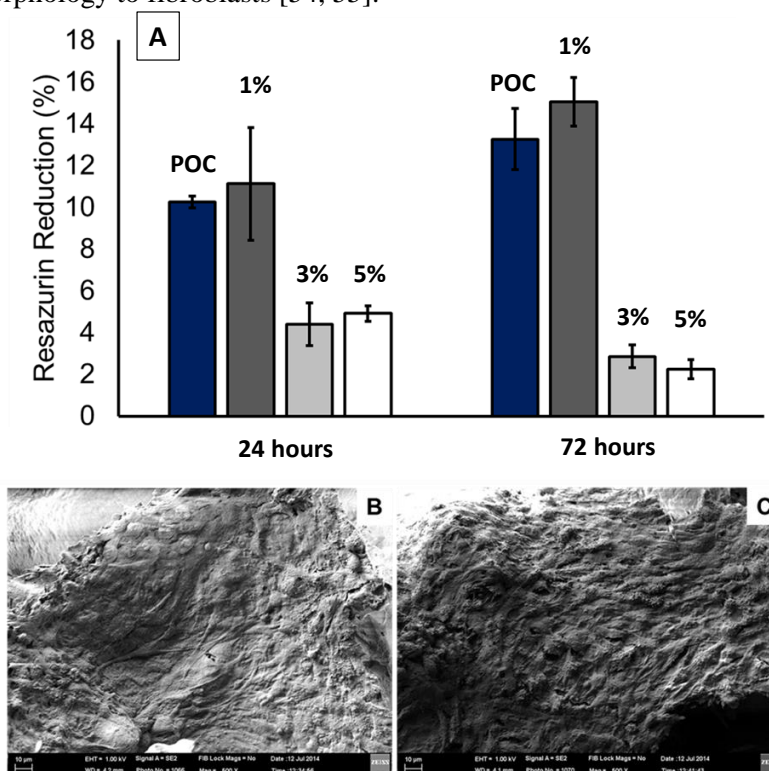


Fig. 10. (A) Resazurin reduction (%) for pure POC and POC-ZnO scaffolds after 24 and after 72 hours. FESEM images of scaffolds after 72 hours in chondrocyte culture: (B) pure POC; and (C) 1% POC-ZnO (bar = 10 μ m).

Our findings revealed that 1% POC-ZnO was a prospective candidate for cartilage tissue engineering, while higher concentration of ZnO will compromise the cell health. Better cell morphology preservation and no cytotoxicity of ZnO NPs in low concentrations can be attributed to the role of ZnO in reactive oxygen species (ROS), anti-inflammatory and wound healing capabilities [48, 56, 57]. It is widely documented that ZnO is a producer of ROS that may damage the cell health at high concentration of ZnO but at low concentrations it is beneficial for cell proliferation [58]. Further research will be required to use similar polymer for various applications by testing different cells with varying percentages of ZnO NP.

4. Conclusion

A new type of nano-composite scaffolds have been produced from citric acid-based polyester and zinc oxide nanoparticles. The scaffolds have been fabricated in two steps: (1) polyesterification synthesis of pre-polymer and mixing with nanoparticles; and (2) production of porous matrix by solvent-casting/particulate-leaching technique. The scaffolds demonstrate elastomeric nature and optimal porosity to be used in tissue engineering applications. Furthermore, our method provides an effective route for production of scaffolds with controlled release of bioactive nanoparticles. Those nanoparticles show strong anti-bacterial properties as evident from our results. The antibacterial activity of the reported scaffolds may enhance the clinical outcomes by following features: (i) reduction of post-operative complications by eliminating the risk of infection from donor; and (ii) reduction of the risk of infection caused by biofilm formation. A multifunctional scaffolds also show a strong potential for cartilage tissue engineering. The concentration of 1 wt% of ZnONP was found to have better performance with chondrocyte proliferation than pure POC, used as control. Our nano-composite scaffold has proven to be optimal for seeding with chondrocytes while simultaneously depleting both the gram positive and gram negative bacteria. This contribution is essential for tissue engineering applications and further studies should not be limited to hard tissue alone. A universal approach can be developed for production of multifunctional scaffolds that would act both as bioactive cellular support and anti-infection agent through controlled release of nanoparticles.

Acknowledgements

This research received funding from University of Malaya IPPP (grant no. PV012 – 2012A) and Ministry of Higher Education (MOHE), Government of Malaysia under the high impact research (UM.C/HIR/MOHE/ENG/44).

References

- [1] Y.-F. Goh, I. Shakir, R. Hussain, *Journal of Materials Science*,. **48**(8), 3027 (2013).
- [2] P. Tran, D. Biswas, A. O'Connor, *Journal of Materials Science*,. **49**(18), 6373 (2014).
- [3] E. Díaz, I. Puerto, I. Sandonis, *International Journal of Polymeric Materials and Polymeric Biomaterials*, **64**(1), 38 (2014).
- [4] E.A. Kamoun, et al., Crosslinked poly(vinyl alcohol) hydrogels for wound dressing applications: A review of remarkably blended polymers. *Arabian Journal of Chemistry*, (0).
- [5] A. Trampuz, W. Zimmerli, *Injury* **37**(2, Supplement) S59 (2006).
- [6] H. Husted, T. Toftgaard Jensen, *Acta Orthop Belg.*, **68**(5), 500 (2002).
- [7] M. Berg-Perier, A. Cederblad, U. Persson, *J Arthroplasty* **7**(4), 457 (1992)
- [8] G.J.Taylor, J.P. Leeming, G.C. Bannister, *J Bone Joint Surg Br.*, **75**(5), 724 (1993)
- [9] A. von Keudell, J.A. Canseco, A.H. Gomoll, *The Journal of Arthroplasty* **28**(6), 918 (2013)
- [10] E.A.,Salvati, et al., *J Bone Joint Surg Am.*, **64**(4), 525 (1982).
- [11] J.W.,Costerton, P.S. Stewart, E.P. Greenberg, *Science*,. **284**(5418), 1318 (1999).
- [12] P.J. Espitia, et al., *Carbohydr Polym* **94**(1), 199 (2013).
- [13] A.K. Zak, , et al., *Materials Letters* **65**(1), 70 (2011).

- [14] R. Wallace, et al., *Journal of Materials Science*, **48**(18): p. 6393 (2013)
- [15] M.I. Khalil, et al., Synthesis and characterization of ZnO nanoparticles by thermal decomposition of a curcumin zinc complex. *Arabian Journal of Chemistry*, (0).
- [16] M.C. Serrano, E.J. Chung, G.A. Ameer, *Advanced Functional Materials* **20**(2), 192 (2010)
- [17] I.Djordjevic, et al., *J Biomater Sci Polym Ed.* **21**(2) 237 (2010).
- [18] I.Djordjevic, *J Biomater Sci Polym Ed.* **21**(8-9), 1039 (2010).
- [19] X.Q.Zhang, et al., *Biomaterials*,. **30**(13). 2632 (2009).
- [20] Qiu, H., et al., *Biomaterials*,. **27**(34) 5845 (2006).
- [21] M.C. Serrano, et al., *Macromolecular Bioscience*,. **11**(5) 700 (2011).
- [22] E.H.M.,Katayoun Kompany, Samira Hosseini, Belinda Pingguan-Murphy, Ivan Djordjevic, *Materials Letters*, 2014.
- [23] I. Djordjevic, et al., *Polymer*,. **50**(7), 1682 (2009).
- [24] J. Yang, A.R. Webb, G.A. Ameer, *Advanced Materials* **16**(6) 511 (2004).
- [25] A. Moradi, et al., *Analytical Methods*,. **6**(12), 4396 (2014)
- [26] D.A.Lee, D.L. Bader, *Journal of Orthopaedic Research*,. **15**(2): p. 181 (1997)
- [27] E.,Parker, et al., *Arthritis Res Ther.* **15**(5): p. R163 (2013).
- [28] E.M. Larson, et al., *Invest Ophthalmol Vis Sci.* **38**(10), 1929 (1997).
- [29] A.,Moradi, et al., *Materials & Design*,. **50**(0) 446 (2013).
- [30] V. Karageorgiou, D. Kaplan, *Biomaterials*,. **26**(27), 5474 (2005).
- [31] Q. Hou, D.W. Grijpma, J. Feijen, *Biomaterials*,. **24**(11), 1937 (2003)
- [32] S.M. Gawish, et al., *Journal of Biomaterials Science, Polymer Edition*, **23**(1-4), 43 (2012).
- [33] S.Vafaei, et al. *Nanotechnology*,. **17**(10), 2523 (2006).
- [34] Athauda, T., et al., *Journal of Materials Science*,. **48**(18), 6115 (2013)
- [35] N. Thadavirul, P. Pavasant, P. Supaphol, *Journal of Biomaterials Science, Polymer Edition*, 2014: p. 1-23.
- [36] A.Thambyah, J.C. Goh, S.D. De, *Med Eng Phys*,. **27**(4), 329 (2005)
- [37] R.A.,Brand, *Iowa Orthop J.* **25**, 82 (2005).
- [38] Y.-B. Luo, et al., *Acta Materialia*,. **57**(11), 3182 (2009).
- [39] Z.X. Meng, et al., *J Nanosci Nanotechnol.* **11**(4), 3126 (2011).
- [40] A.Moezzi, A.M. McDonagh, M.B. Cortie, *Chemical Engineering Journal*,. **185–186**(0), 1 (2012).
- [41] G. Colon, B.C. Ward, T.J. Webster, *J Biomed Mater Res A*, **78**(3), 595 (2006).
- [42] J.Yang, et al., *Biomaterials*,. **27**(9), 1889 (2006).
- [43] H.S.Shirazi, et al., *Progress in Organic Coatings*,. **77**(4), 821 (2014).
- [44] A. Hahn, et al., *J Control Release*,. **154**(2), 164 (2011)
- [45] T. Jin, et al., *J Food Sci.* **74**(1) M46-52. 2009
- [46] L., Zhang, et al., *Journal of Nanoparticle Research*,. **9**(3), 479 (2007)
- [47] A.S. Prasad, et al., *American Journal of Clinical Nutrition*,. **85**(3), 837 (2007)
- [48] A.S. Prasad, *Experimental Gerontology*,. **43**(5), 370 (2008)
- [49] E. Ho, C. Courtemanche, B.N. Ames, *Journal of Nutrition*,. **133**(8), 2543 (2003).
- [50] S.Yang, et al., *Materials & Design*,. **59**(0), 461 (2014).
- [51] P. Feng, et al., *PLoS ONE*,. **9**(1), e87755 (2014).
- [52] P. Dwivedi, et al., *International Journal of Polymeric Materials and Polymeric Biomaterials*, **63**(16), 859 (2014)
- [53] K.R. Brodtkin, A.J. García, M.E. Levenston, *Biomaterials*,. **25**(28), 5929 (2004)
- [54] K. Na, et al., *Biotechnology Letters*, **29**(10), 1447 (2007).
- [55] L. Gutwein, T. Webster, *Journal of Nanoparticle Research*,. **4**(3), 231 (2002).
- [56] A. Kumar, et al., *Free Radical Biology and Medicine*,. **51**(10), 1872 (2011)
- [57] C. Lang, et al., *American Journal of Physiology-Lung Cellular and Molecular Physiology*, **292**(2), L577 (2007).
- [58] R. Augustine, et al., *Journal of Polymer Research*, **21**(3), 1 (2014).